International Journal of Mass Spectrometry 279 (2009) 76–81

Contents lists available at ScienceDirect

International Journal of Mass Spectrometry

journal homepage: www.elsevier.com/locate/ijms

Penning ionization in the electron beam assisted secondary ion mass spectrometry-dependence of ionization potential

Wei-Chiang Lee, J. Hwang*

Department of Materials Science and Engineering, National Tsing Hua University, Hsinchu, Taiwan

ARTICLE INFO

Article history:
Received 12 May 2008
Received in revised form 4 October 2008
Accepted 6 October 2008
Available online 19 October 2008

Keywords:
Secondary ion mass spectrometry
Ion-solid interactions
Penning ionization
Ionization potential

ABSTRACT

The enhancement of secondary ion signals has been investigated for the Si(1 0 0) wafers implanted with different chemical elements using the electron beam assisted secondary ion mass spectrometry (SIMS). The $^{7}Li^{+}$, $^{40}Ca^{+}$, $^{50}Ti^{+}$, $^{24}Mg^{+}$, $^{11}B^{+}$ and $^{30}Si^{+}$ secondary ion signals increase linearly with electron beam current at different rates, supported by the SIMS depth profiles. An enhancement factor (*e*-factor) is defined to characterize the increased percentage of a secondary ion signal. The $^{7}Li^{+}$, $^{40}Ca^{+}$, $^{50}Ti^{+}$, $^{24}Mg^{+}$, $^{11}B^{+}$ and $^{30}Si^{+}$ secondary ion signals exhibit *e*-factors of 0.1, 1.6, 6.1, 26.4, 59.2 and 71.4%, respectively at an electron beam current of 90 μA. The *e*-factor increases in an exponential function with ionization potential. A proposed Penning ionization mechanism on the sample surface can well explain the experimental results. The Penning ionization is dominated by the oxygen radicals since no secondary ion enhancements were observed when the O_2^{+} primary ion was replaced by Cs^{+} in SIMS operations.

1. Introduction

Secondary ion mass spectrometry (SIMS) has attracted much attention in the electronic industry because of its ultra-high sensitivity. The sensitivity of SIMS is directly correlated to the secondary ion yields of chemical elements that are usually enhanced by optimizing instrumental parameters such as primary beam ions, primary beam energy, and angle of incidence. Other techniques such as post acceleration, post ionization and gas flooding have been demonstrated to enhance the secondary ion yield [1–4]. Recently, we have reported the enhancement of secondary ion yield by the assistance of electron beam in a SIMS operation [5]. An electron beam is incident normally onto the BF_2^{+} implanted Si(1 0 0) surface during the O_2^{+} ion bombardment in a SIMS operation. The $^{11}B^{+}$ ion signal increases linearly with electron beam current. The energy spectra of $^{11}B^{+}$ support that the enhancement of $^{11}B^{+}$ is contributed from the ionization on the sample surface.

In this paper, we present the dependence of chemical elements on the secondary ion yield enhancement in the electron beam assisted SIMS operations. From a fundamental view, the interaction among electrons, detected chemical elements and O_2^{+} ions are very complex. The $^{7}Li^{+}$, $^{40}Ca^{+}$, $^{50}Ti^{+}$, $^{24}Mg^{+}$, $^{11}B^{+}$ and $^{30}Si^{+}$ ions are chosen to illustrate the dependence of chemical elements on the ionization enhancement. Experimental results support that secondary positive ion yields increase exponentially with ionization potential. The Penning ionization mechanism is very suitable for explaining the depth profiles and the energy spectra of $^{7}Li^{+}$, $^{40}Ca^{+}$, $^{50}Ti^{+}$, $^{24}Mg^{+}$, $^{11}B^{+}$ and $^{30}Si^{+}$ ions.

2. Experimental procedures

A P-type Si(1 0 0) wafer was implanted with ^{7}Li, ^{40}Ca, ^{50}Ti, ^{24}Mg and ^{11}B ions at 50, 200, 200, 150 and 80 KeV with dosages of 1.15×10^{14}, 0.97×10^{14}, 1.0×10^{14}, 1.14×10^{14} and 1.044×10^{14} at./cm^2. The as-implanted p-Si(1 0 0) wafer was fed into a magnetic sector mass spectrometer (CAMECA IMS-6f), equipped with an electron gun originally designed for charge neutralization. The electron gun was tuned to supply energetic electrons that were able to enhance the ionization yield during the SIMS measurement. The energy of the O_2^{+} source was set at 10 KeV and biased at 4.5 KV in order to keep the incident angle of the O_2^{+} primary ions around 45 degrees from surface normal. In the depth profile measurements, the primary O_2^{+} ion beam was raster-scanned across a raster area of 120 μm × 120 μm at ~75 nA. The electron gun was biased at −4.5 KV such that the energy of electrons was 9 KeV relative to the sample. The electron beam current varying from 0 to 90 μA was normally incident onto the sample surface in the ionization process. A series of ^{7}Li, ^{40}Ca, ^{50}Ti, ^{24}Mg, ^{11}B and ^{30}Si ion depth profiles were taken to characterize the efficiency of the ionization process assisted by the electron beam.

* Corresponding author at: National Tsing Hua University, Department of Materials Science and Engineering, 101, Section 2, Kuang-Fu Road, Hsinchu 30013, Taiwan.
E-mail address: jch@mx.nthu.edu.tw (J. Hwang).

1387-3806/$ – see front matter © 2008 Elsevier B.V. All rights reserved.
doi:10.1016/j.ijms.2008.10.004

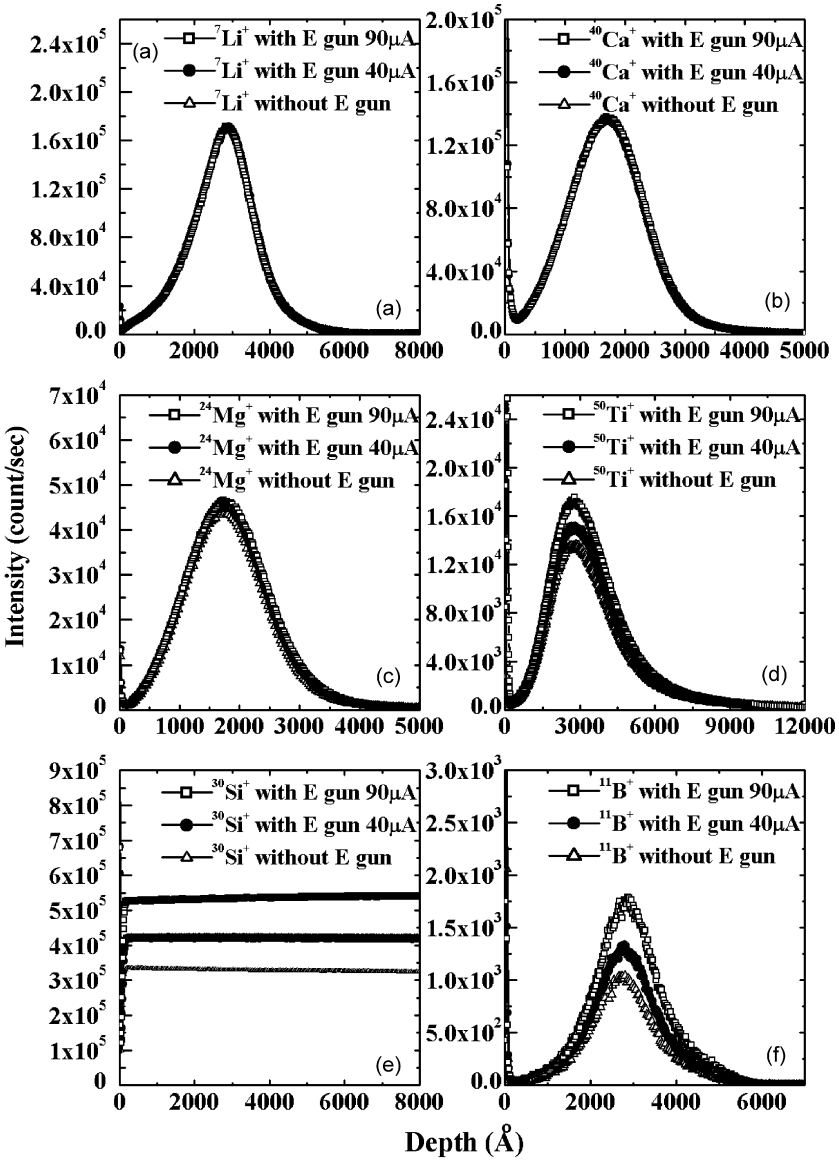

Fig. 1. Linear plots of positive secondary ion depth profiles in the electron beam assisted SIMS operations for the Si(1 0 0) samples implanted with Li, Ca, Ti, Mg, and B of different dosages. The detected secondary ions and the ion implantation conditions are (a) $^{7}Li^{+}$, 50 KeV, 1.15×10^{14} at./cm^2, (b) $^{40}Ca^{+}$, 200 KeV, 0.97×10^{14} at./cm^2, (c) $^{50}Ti^{+}$, 200 KeV, 1.0×10^{14} at./cm^2, (d) $^{24}Mg^{+}$, 150 KeV, 1.14×10^{14} at./cm^2, (e) $^{30}Si^{+}$, from silicon matrix, and (f) $^{11}B^{+}$, 80 KeV, 1.044×10^{14} at./cm^2. The ion beam current and ion voltage of the O_2^{+} primary ion source are 75 nA and 5.5 KeV, respectively for all the SIMS experiments. The operation conditions of electron beam are 40 and 90 μA and 9 KeV relative to the Si sample.

3. Results and discussion

3.1. In-depth analysis under O_2^{+} bombardment with and without electron beam on

Secondary ion signals can be enhanced in a SIMS operation by an electron beam concurrently incident onto the sample during ion bombardment. The enhancement of secondary ion signals depends on the type of chemical elements, which is clearly illustrated in the in-depth profiles of $^{7}Li^{+}$, $^{40}Ca^{+}$, $^{50}Ti^{+}$, $^{24}Mg^{+}$, $^{30}Si^{+}$ and $^{11}B^{+}$ shown in Fig. 1(a–f). The increases of the $^{7}Li^{+}$, $^{40}Ca^{+}$, $^{50}Ti^{+}$, $^{24}Mg^{+}$, $^{30}Si^{+}$ and $^{11}B^{+}$ signals can be quantified by the enhancement factor (*e*-factor) that is defined as:

$$e = \frac{h_1 - h_2}{h_2} \times 100\%$$

where h_1 is the enhanced signal with electron beam on and h_2 is the original signal with electron beam off [6]. The *e*-factors of the $^{7}Li^{+}$, $^{40}Ca^{+}$, $^{50}Ti^{+}$, $^{24}Mg^{+}$, $^{30}Si^{+}$ and $^{11}B^{+}$ signals increase with electron beam current as shown in Fig. 2. Different ion exhibits different enhancement rate that characterizes the increase of *e*-factor per unit current. The increase sequence of the enhancement rate is $^{7}Li^{+}$, $^{40}Ca^{+}$, $^{50}Ti^{+}$, $^{24}Mg^{+}$, $^{30}Si^{+}$ and $^{11}B^{+}$ in our study. From a chemical view, ionization is an energy transfer process that requires activation energy high enough to overcome the ionization potential. Deline et al. have shown that an exponential relationship exists between positive ion yield and ionization potential [7,8]. The variation of the enhancement rate for different ion is thus attributed to different ionization potential. The *e*-factor increases in an exponential function with the ionization potential as shown in Fig. 3. For a chemical element with higher ionization potential, the *e*-factor of the secondary ion is higher. The exponential relationship between *e*-factor and ionization potential Q_M for a chemical element M can

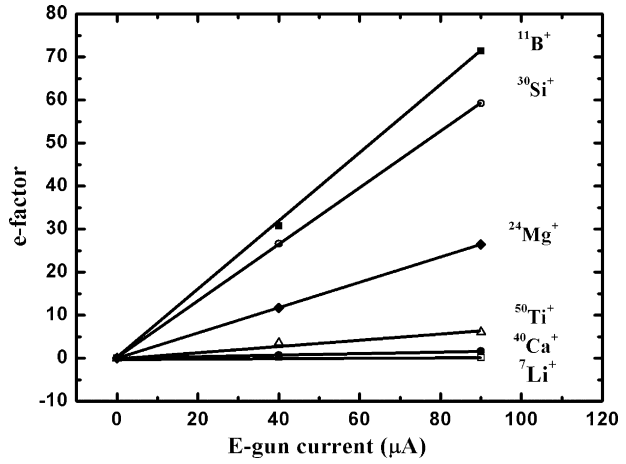

Fig. 2. Enhancement factors for the ^{7}Li, ^{40}Ca, ^{50}Ti, ^{24}Mg, ^{11}B and ^{30}Si signals as a function of electron beam current in the electron beam assisted ionization process.

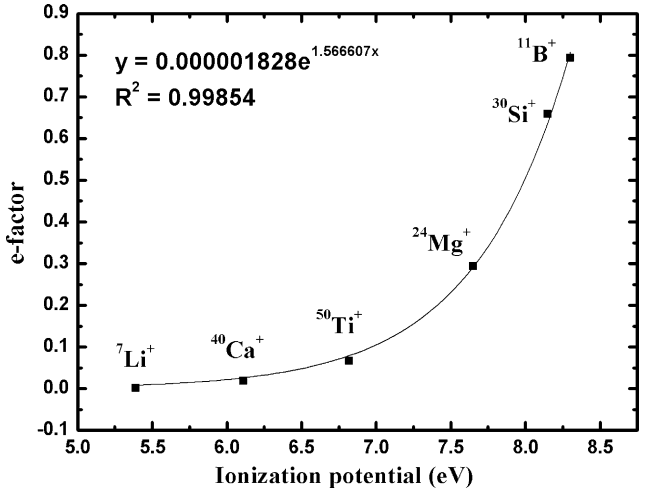

Fig. 3. Relationship between the enhancement factors and the ionization potentials of chemical elements. The *e*-factor increases in an exponential function with ionization potential.

be expressed as:

$$e = Ae^{mQ_M}$$

where the pre-exponential constant A is 1.83E-6 and the exponential constant m is 1.57 from the curve-fit result in Fig. 3.

3.2. Penning ionization

Penning ionization can well explain the depth profile data of $^{7}Li^+$, $^{40}Ca^+$, $^{50}Ti^+$, $^{24}Mg^+$, $^{30}Si^+$ and $^{11}B^+$ in Fig. 1(a–f) and the *e*-factor data in Figs. 2 and 3. Penning ionization characterizes the reaction on the sample surface involving oxygen radicals O_2^*, which is sketched in Fig. 4 and is described in reaction (1) below [9–12].

$$O_2^* + M \rightarrow O_2 + M^+ + e^- \quad (1)$$

where O_2^* denotes the oxygen radical, M is the matrix atom, O_2 is the oxygen molecule, M^+ is the ion from matrix, and e^- is the electron. The reaction rate r_1 in reaction (1) is expressed as:

$$r_1 = \frac{d[M^+]}{dt} = k_1[O_2^*][M]$$

The generation of M^+ ion is proportional to the concentrations $[O_2^*]$ and [M].

The electron beam can excite neutral O_2 molecules to their radical O_2^* states for Penning ionization according to reaction (2) below:

$$O_2 + e^- \rightarrow O_2^* + e^- \quad (2)$$

The ground state of an O_2 molecule is triplet that is treated as a neutral O_2 molecule here. And any excited state of an O_2 molecule is treated as an O_2 radical. The reaction rate r_2 is proportional to the concentrations $[O_2]$ and $[e^-]$ and is expressed as:

$$r_2 = \frac{d[O_2^*]}{dt} = k_2[O_2][e^-]$$

where k_2 is a constant. Since the electron concentration $[e^-]$ is proportional to electron beam current, the rate constant r_2 becomes:

$$r_2 = \frac{d[O_2^*]}{dt} = k_2'[O_2]I_e$$

where I_e is the electron beam current and k_2' is the new constant. The generation rate of O_2^* radicals, i.e., $d[O_2^*]/dt$, is thus proportional to electron current I_e. Taking into account the reactions (1)

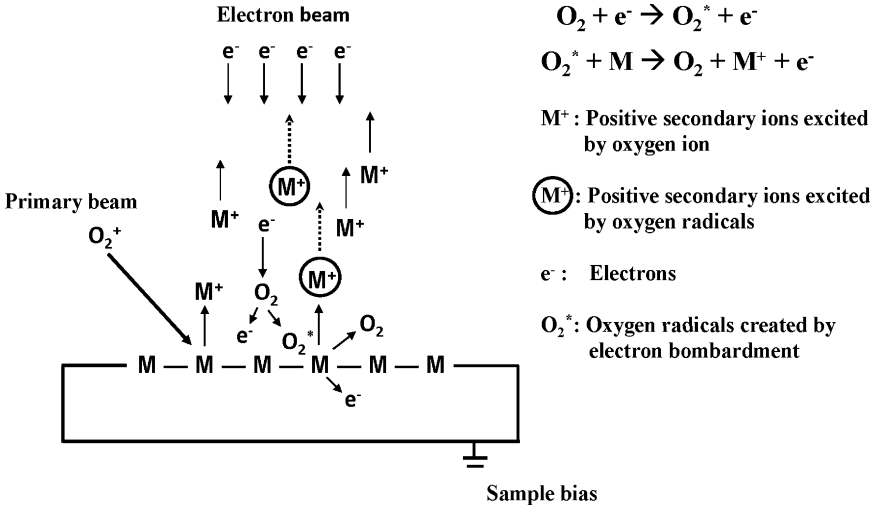

Fig. 4. Schematic diagram showing the ionization of Li, ^{40}Ca, ^{50}Ti, ^{24}Mg, ^{11}B or ^{30}Si by the Penning ionization mechanism induced by electron beam.

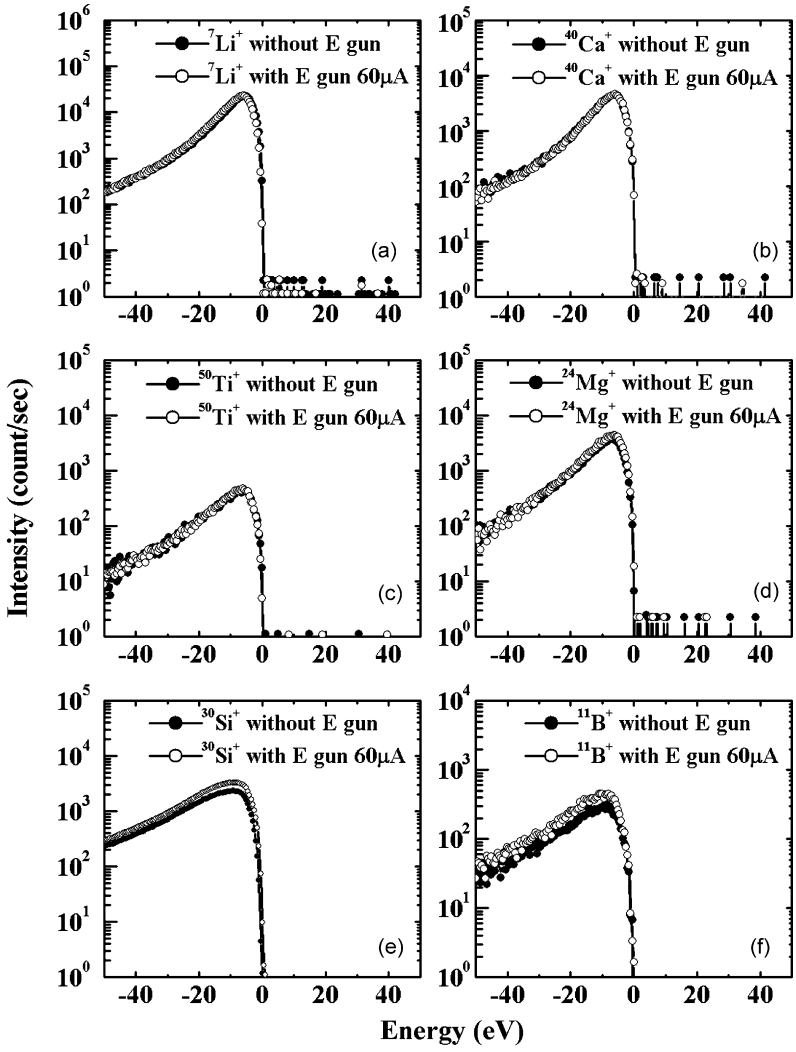

Fig. 5. Energy spectra of the secondary ions from ion implanted Si(1 0 0) samples in SIMS operations with electron gun off and on: (a) $^{7}Li^{+}$, (b) $^{40}Ca^{+}$, (c) $^{50}Ti^{+}$, (d) $^{24}Mg^{+}$, (e) $^{30}Si^{+}$ and (f) $^{11}B^{+}$. The electron gun is operated at 9 KV and 60 μA. The primary ion O_2^{+} is operated at 5.5 KeV and 50 nA.

and (2), the generation of M^{+} ion, i. e. $d[M^{+}]/dt$, is also proportional to electron beam current I_e. This is in good agreement with the depth profile data of $^{7}Li^{+}$, $^{40}Ca^{+}$, $^{50}Ti^{+}$, $^{24}Mg^{+}$, $^{11}B^{+}$ and $^{30}Si^{+}$ in Fig. 2, supporting that the O_2^{*} radicals play important roles in the enhancement of ionization efficiency.

Considering a regular SIMS process,

$$O_2^{+} + M \rightarrow O_2 + M^{+} \quad (3)$$

where O_2^{+} is the oxygen ion from the primary source, M is the matrix atom, O_2 is the oxygen molecule, and M^{+} is the ion from the matrix. The SIMS process is a simple collision process with energetic O_2^{+} ions through which the matrix atoms M can be ionized into M^{+} ions. The generation rate of M^{+} ions is defined as r_3 that can be expressed as:

$$r_3 = \frac{d[M^{+}]}{dt} = k_3 I_{O_2^{+}}[M]$$

The *e*-factor is defined as the enhanced percentage of the secondary ion signal. According to the proposed Penning ionization, the *e*-factor equals to $[(r_3 + r_1) - r_3]/r_3$ based on the reactions (1) and (3). Considering the ionization in an impact process in the reactions (1) and (3), the reaction rates r_1 and r_3 depend on ionization potential, ion energy, electron energy and incident orientation. To first order of approximation, the *e*-factor for the chemical element M can be further derived by taking into account the effect of ionization potential and is expressed as:

$$e = \frac{r_1}{r_3} = \frac{k_1[O_2^{*}][M]}{k_3 I_{O_2^{+}}[M]} = \frac{k_1[O_2^{*}]}{k_3 I_{O_2^{+}}} = \frac{k_{1M} e^{-c_1 Q_M}[O_2^{*}]}{k_{3M} e^{-c_3 Q_M} I_{O_2^{+}}}$$

$$= \frac{k_{1M}[O_2^{*}]}{k_{3M} I_{O_2^{+}}} e^{(c_3 - c_1)Q_M}$$

where the rate constants k_1 and k_3 are considered inversely exponential to the ionization potential Q_M and (K_{1M}, K_{3M}) and (c_1, c_3) are the corresponding pre-exponential and exponential constants, respectively. Note that the factors c_1 and c_3 are not equal since the Eqs. (1) and (3) are different. From a theoretical consideration, the factors c_1 and c_3 are influenced by the experimental parameters such as electron energy, ion energy, and incident direction. The factors c_1 and c_3 are fixed in all the experiments.

As mentioned earlier, the generation rate of O_2^{*} radicals, i.e., $d[O_2^{*}]/dt$ is proportional to electron beam current I_e. The concentration $[O_2^{*}]$ is thus proportional to the electron beam irradiation time t. In an electron beam assisted SIMS operation, the electron

beam current is fixed. The $[O_2^*]$ can be expressed as:

$$[O_2^*] = \int k_2'[O_2]I_e dt = I_e \int k_2'[O_2]dt$$

Therefore the *e*-factor becomes:

$$e = \frac{k_{1M}I_e \int k_2'[O_2]dt}{k_{3M}I_{O_2^+}} e^{(c_s - c_1)Q_M}$$

The *e*-factor is proportional to the electron beam current I_e and in an exponential function of ionization potential Q_M, as what observed in Figs. 2 and 3.

3.3. Considerations on the proposed Penning ionization

3.3.1. Penning ionization involving oxygen radicals O_2^*

We present that secondary ion signals can be enhanced in a SIMS operation with electron gun on. The enhanced secondary ion signals may result from O_2^* radical generation ($O_2 + e^- \rightarrow O_2^* + e^-$) and Penning ionization ($O_2^* + M \rightarrow O_2 + M^+ + e^-$) near the sample surface. The source of O_2 molecules for the O_2^* radicals generation is from the primary oxygen ions, rather than the residual oxygen gas in the SIMS chamber under UHV condition. There are two possible ways to generate O_2 molecules source near the sample surface. First, the primary O_2^+ ions can be neutralized into O_2 molecules during primary ion bombardment onto the sample surface and then backscatter from the sample surface. Second, it is possible that the implanted oxygen is re-sputtered out of surface in a form of O_2 molecules. The O_2 molecules near the sample surface probably interact with incident electrons and are excited into O_2^* radicals for Penning ionization.

The Penning ionization involves oxygen radicals O_2^*, rather than other chemical species, in reaction (1). This can be supported by performing similar SIMS experiments by replacing the O_2^+ primary ion source with the Cs^+ ion source. If no secondary ion enhancement occurs for the Cs^+ primary ion source, this tends to support the role of oxygen in the Penning ionization process. Fig. 5 shows the depth profiles of $11B^+$ and $28Si^+$ collected using the Cs^+ primary ion source for a shallow p/n junction implanted with BF_2^+ at 20 KeV with a dosage of $2.3 \times 1015\,cm^{-2}$. No secondary ion enhancement occurs for both $11B^+$ and $28Si^+$ ions. This support the role of oxygen involved in the Penning ionization process. In a SIMS operation using Cs+ primary ion source, negative secondary ions usually exhibit higher count rate than positive secondary ions. However, positive secondary is of interest in the Penning ionization. The highly doped boron Si(1 0 0) samples are used such that the positive secondary ion signal can be clearly observed.

In order to further confirm the role of oxygen in the secondary ionization enhancement, we also perform SIMS measurements at various primary O_2^+ ion beam currents. The enhancement of secondary ion signals (B^+, Si^+) indeed occur at various primary O_2^+ ion beam currents when electron beam current is on. The enhancement of secondary ion signals increases with increasing primary O_2^+ ion beam current, as shown in Fig. 6. This reasonable since the amounts of O_2 molecules and O_2^* radicals near the sample surface are expected to increase with primary O_2^+ ion beam current.

3.3.2. Penning ionization on the Si surface supported by energy spectra

Fig. 5(a–f) show the energy spectra of secondary ions $^7Li^+$, $^{40}Ca^+$, $^{50}Ti^+$, $^{24}Mg^+$, $^{30}Si^+$ and $^{11}B^+$ from ion implanted Si(1 0 0) samples in SIMS operations with electron gun off and on. The electron gun is operated at 9 KV and 60 μA. The primary ion O_2^+ is operated at 5.5 KeV and 50 nA. With electron gun off, the maximum peak of $^7Li^+$ appears approximately at −6 eV in the energy spectra in

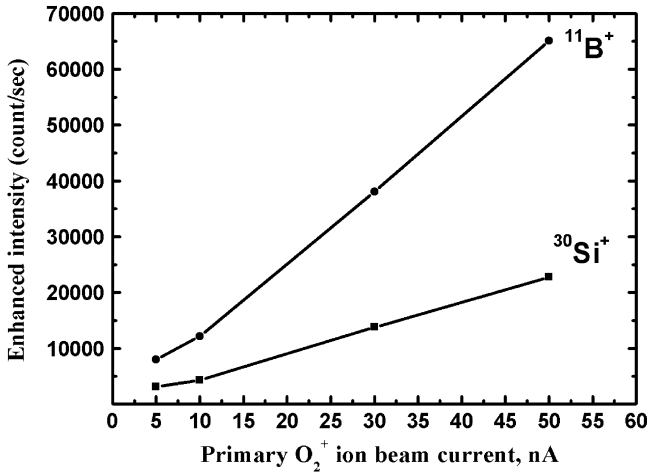

Fig. 6. Enhanced secondary ion intensities of $^{11}B^+$ and $^{30}Si^+$ at different primary O_2^+ ion beam current conditions. The secondary ion signal enhancement occurs since an electron beam current of 60 μA is incident onto the sample surface in SIMS operations.

Fig. 5(a). This indicates that most $^7Li^+$ ions right after desorption on the surface exhibit a kinetic energy of 6 eV. From a chemical perspective, the kinetic energy of 6 eV enables Li ions to overcome the surface energy barrier in order to escape from the Si(1 0 0) surface. When the electron gun is on, the $^7Li^+$ peak remains unchanged. No peak shift of $^7Li^+$ suggests that the possible charging induced effects can be neglected in our SIMS operations. Moreover, no $^7Li^+$ signal appears on the positive energy side in Fig. 5(a). The secondary ion signal on the positive energy side in the energy spectra characterizes the intensity of ions at a position above the sample surface [13]. The $^7Li^+$ data supports that the detected $^7Li^+$ ions are from the Si surface, rather than from a position above the Si surface. This agrees very well with the proposed Penning ionization occurred on the sample surface. Similarly, all the other secondary ions $^{40}Ca^+$, $^{50}Ti^+$, $^{24}Mg^+$, $^{30}Si^+$ and $^{11}B^+$ do not have signals on the positive energy side in the energy spectra in Fig. 5(b–f). This supports that all the detected ions are from the Si surface in agreement with the proposed Penning ionization. The differences among the detected secondary ions in Fig. 5(a–f) are their maximum peak position and their relative peak intensity. In particular, both $^{30}Si^+$ and $^{11}B^+$ signals are clearly enhanced when the electron gun is on. This is in good agreement with the depth profile data of $^{30}Si^+$ and $^{11}B^+$ in Fig. 1(e and f).

3.3.3. Possibility of the secondary ion enhancement induced by charging or thermal effects

Two possible ways to affect secondary ion ionization in SIMS measurements are thermal and charging effects when electron beam current is on. The charging effect does not occur in our cases since the energy spectra in Fig. 5 show no charging for various experimental conditions. The temperature is expected to increase in the electron beam assisted SIMS operation. The possibility of the secondary ion enhancement by means of increasing the sample temperature is excluded based on the following argument. If the thermal effect dominated the secondary ion ionization enhancement, we would observe the same enhancement effect for the SIMS experiment using the Cs^+ primary ion source. However, no secondary ionization enhancement was observed for the SIMS experiments using Cs^+, as shown in Fig. 7. The thermal effect is thus considered not able to affect the ionization enhancement in our experiment.

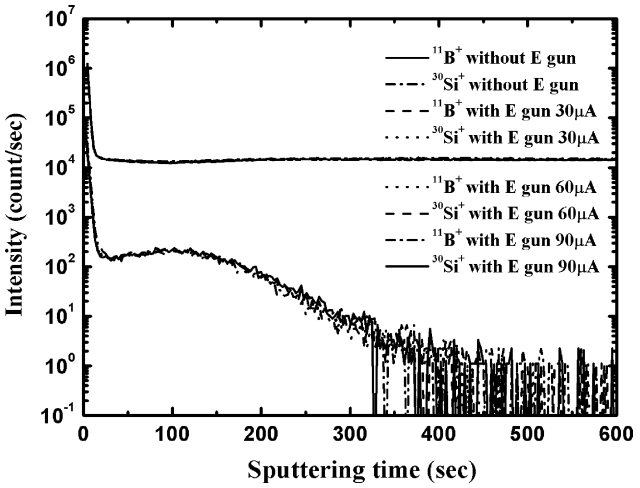

Fig. 7. The SIMS depth profiles of $^{11}B^+$ and $^{28}Si^+$ in a shallow p/n junction implanted with BF_2^+ at 20 KeV with a dosage of 2.3×10^{15} cm^{-2}. The SIMS experiments were performed using the Cs^+ primary ion source of 2 KeV with electron flooding. The electron beam energy is 6.5 KeV relative to the Si sample.

No observation of secondary ionization enhancement for the SIMS experiments using Cs^+ can be well explained based on the following arguments. First, Cs^+ implantation would have the effect of lowering the work function of Si. Therefore, no charging effect would occur to affect secondary ion signals. Second, Penning ionization involves oxygen radicals according to the Eq. (1). However, no oxygen molecules or radicals can be generated near the sample surface when the primary ion is Cs^+. Third, no signal enhancement implies that the possible secondary ion enhancement by means of thermal effect is excluded.

4. Conclusion

The enhancement of secondary ion signals occurs for the Si(1 0 0) wafers implanted with $^7Li^+$, $^{40}Ca^+$, $^{50}Ti^+$, $^{24}Mg^+$ or $^{11}B^+$ ions by the assistance of electron beam in SIMS operations. The secondary ionization enhancement increases linearly with electron beam current. The secondary ion enhancement increases exponentially with ionization potential. For a chemical element with higher ionization potential, the secondary ion enhancement is higher. Penning ionization on the sample surface can well explain the dependence of ionization potential on the secondary ion enhancement.

Acknowledgements

The authors would like to thank Dr. A. Merkulov and Dr. P. Peres (CAMECA France Co., Ltd) for helpful advices in tuning the electron gun. The valuable discussions with Dr. S. Biswas (Cascade Scientific Ltd.) and Mr. C. F. Chang are appreciated.

References

[1] R. Liu, C.M. Ng, A.T.S. Wee, Ultra shallow secondary ion mass spectrometry, Solid-State Integrated-Circuit Technol. (2001), http://ieeexplore.ieee.org.
[2] A. Benninghoven, F.G. Rudenauer, H. Werner, Secondary Ion Mass Spectrometry: Basic Concepts, Instrumental Aspects, Applications and Trends, John Wiley & Sons, New York, 1987.
[3] W. Reuter, Anal. Chem. 59 (1987) 2081.
[4] Y. Gao, H.N. Migeon, M. Juhel, J. Lecart, Surf. Interf. Anal. 20 (1993) 716.
[5] Wei-Chiang Lee, J. Hwang, Int. J. Mass Spectrom. 274 (2008) 25–29.
[6] J. Sielanko, J. Filiks, M. Sowa, J. Zinkiewicz, M. Drewniak, Vacuum 46 (1995) 1459.
[7] V.R. Deline, C.A. Evans Jr., P. Williams, Appl. Phys. Lett. 33 (1978) 578.
[8] B.G. Wilson, F.A. Stevie, C.W. Magee, Secondary Ion Mass Spectrometry, John Wiley & Sons, 1989, p. 3.3-1.
[9] A. Corney, O.M. Williams, J. Phys. B: Atom. Molec. Phys. 5 (1972) 686.
[10] P.E. Siska, Rev. Modern Physics 65 (1993) 337.
[11] R.L. Sharpless, T.G. Slanger, J. Chem. Phys. 91 (1989) 7947.
[12] B. Carol Johnson, Peter L. Smith, R.D. Knight, Astrophysical J. 281 (1984) 477.
[13] Berta Guzman de la mat, Mark G. Dowett, Ion and electron bombardment-related ion emission during the analysis of diamond using secondary ion mass spectrometry, J. Appl. Phys. 101 (2007), 034910-1–034910-5.